THERMAL SHIELD SUPPORT DEGRADATION IN PRESSURIZED WATER REACTORS*

CONF-860722--18

TI86 013397

by

F. J. Sweeney
D. N. Fry

Oak Ridge National Laboratory
Oak Ridge, Tennessee 37831

Paper submitted to the
Symposium on Special Topics of Structural Vibration
American Society of Mechanical Engineers
Pressure Vessel and Piping Conference
July 20-26, 1986
Chicago, Illinois

*Research sponsored by the U.S. Nuclear Regulatory Commission under Interagency Agreement No. 40-551-75 and performed at Oak Ridge National Laboratory, operated by Martin Marietta Energy Systems, Inc., for the U.S. Department of Energy under Contract No. DE-AC05-84OR21400.

ABSTRACT

Damage to the thermal shield support structures of three pressurized water reactors (PWRs) due to flow-induced vibrations was recently discovered during refueling. In two of the reactors, severe damage occurred to the thermal shield, and in one reactor the core support barrel (CSB) was damaged, necessitating extended outages for repairs. In all three reactors, several of the thermal shield supports were either loose, damaged, or missing. The three plants had been in operation for approximately 10 years before the damage was apparent by visual inspection.

Because each of the three U.S. PWR manufacturers have experienced thermal shield support degradation, the Nuclear Regulatory Commission requested that Oak Ridge National Laboratory analyze ex-core neutron detector noise data to determine the feasibility of detecting incipient thermal shield support degradation. Reactor manufacturers and utilities provided the noise data for the analysis. Finite element model calculations were also performed to predict changes in the vibrational responses of core internal structures under degraded thermal shield support conditions.

Results of the noise data analysis indicate that thermal shield support degradation probably began early in the life of both severely damaged plants. The degradation was characterized by shifts in the resonant frequencies of core internal structures and the appearance of new resonances in the ex-core neutron detector noise. Both the data

analyses and the finite element calculations indicate that these changes in resonant frequencies are less than 3 Hz.

We concluded from the study that a well planned reactor vibration and neutron noise analysis program combined with theoretical calculations could aid structural design, performance verification, and monitoring of reactor internals undergoing flow-induced vibrations.

NOMENCLATURE

$NCPSD_{12}$ = cross power spectral density magnitude normalized to the mean (dc) levels of signals 1 and 2, 1/Hz

$NPSD_1$ = power spectral density normalized to the mean (dc) level squared of signal 1, 1/Hz

coherence = $(NCPSD_{12})^2/(NPSD_1 \times NPSD_2)$, unitless

INTRODUCTION

Every reactor type (including gas- and liquid metal-cooled reactors) has experienced degradation of reactor internal structures due to flow-induced vibrations (1-3). These degradations are of great financial concern because of the high cost (up to one million dollars per day) of replacement power and capital investment. From a safety standpoint, degradation of internal structures can threaten the integrity of the first and second levels of radioactivity containment in the reactor system (the fuel cladding and primary coolant system respectively) through the generation of loose parts. As a result of these experiences, the U.S. Nuclear Regulatory Commission (NRC) has required loose part monitoring systems (LPMS) on reactors licensed since 1975 (4).Many pressurized water reactors (PWRs) also monitor core internals vibrations through spectrum analysis of ex-core (2) (outside the reactor pressure vessel) or in-core (5) neutron detector signals (neutron noise).

Recently, the thermal shields (Figs. 1 and 2) of two Combustion Engineering (CE) PWRs (henceforth referred to as reactor A and reactor B) were found to have sustained extensive damage as a result of flow-induced vibrations. This damage consisted of cracks in the thermal shield and loss of or damage to lateral support pins. In both plants, loose parts were generated in the primary system, and in one of the reactors (reactor A), damage also occurred to the core support barrel (CSB). The two plants had been in commercial operation for approximately 10 years (5 fuel cycles) and had undergone required in-service inspections (ISI) prior to discovery of the damage. The thermal shields of these two plants have since been removed, necessitating outages for repair of up to one year.

Loose thermal shields or degraded supports have also occurred in other CE, Babcock and Wilcox (B&W), and Westinghouse PWRs. In some plants, however, the thermal shield is necessary to prevent radiation-induced weakening of the pressure vessel welds. In these cases, reactor operation without a thermal shield would not be allowed because of pressurized thermal shock (PTS) limitations.

Because reactors built by each of the three U.S. PWR manufacturers have experienced thermal shield support degradation, the NRC requested that Oak Ridge National Laboratory analyze ex-core neutron detection noise data from reactors with and without degraded thermal shield supports. Data supplied by reactor manufacturers and utilities was utilized to determine the feasibility of detecting incipient thermal shield support degradation. Finite element model calculations were also performed to predict changes in the vibrational responses of core internal structures under degraded thermal shield support conditions.

FINITE ELEMENT CALCULATIONS

Five finite element models of the reactor core and core support structures for a typical PWR were studied.[1] Each of these models includes a half-symmetric representation of the core and core support structure system as shown in Fig. 3. The model shown in Fig. 3 represents the baseline case and includes the core barrel, core liner, thermal shield, plenum and lower grid, a simulated fuel assembly representation, and a full complement of attachments between the core barrel and thermal shield.

---

[1]The analyses were performed by SAIC, Inc., on a plant whose structural details were available to us. The thermal shield supports are different from those of the specific CE plants for which neutron noise data was available.

The other four models represent variations on this baseline case and simulate various forms of thermal shield support degradation: upper radial attachments missing over a 60 deg sector, no upper radial attachment, degraded lower attachment with no upper attachment, and no thermal shield. Schematic representations of these cases are presented in Fig. 4.

The PAFEC (6) computer code was used to perform the structural analyses for the study. Natural frequencies and normal mode shapes of the core internal structures in water were determined for the five models presented. Table 1 presents a summary of the natural frequencies and mode shapes of the core barrel and thermal shield.[2] The fuel assembly bending mode frequency was fixed in the models at 3.47 Hz.

The results predict the following behavior of core internals vibrations:

1. In the baseline (undegraded) case, the core barrel and thermal shield do not act independently (i.e., they vibrate as a unit).

2. Changes in the CSB/thermal shield beam (pendular) mode frequency are small (<1.5 Hz) even for severely degraded thermal shield attachments including the case in which the

---

[2]No attempt was made to adjust the model parameters (other than the fuel assembly bending mode frequency) to produce frequencies matching neutron noise results.

thermal shield was removed. The CSB/thermal shield shell mode changed <3 Hz.

3. Degradation of the thermal shield supports can lead to either increases or decreases in the CSB/thermal shield beam-mode frequency. The direction of the frequency change is dependent upon the relative importance of stiffness and effective mass changes due to support degradation. When upper attachments are degraded, the CSB/thermal shield system becomes less stiff leading to a decrease in its resonant frequency. When both upper and lower attachments are degraded, the effective mass of the system is reduced. This reduction in effective mass leads to an increase in the beam-mode frequency. Increases in the beam mode frequency usually occur after the thermal shield supports become severely degraded.

4. Degradation of both upper and lower attachments leads to the appearance of independent thermal shield shell modes. These vibrations occur at frequencies lower than the shell mode of the combined CSB/thermal shield system.

EX-CORE NEUTRON DETECTOR NOISE DATA OBSERVATIONS

Reactor manufacturers and utilities supplied ORNL with neutron noise data in the form of plots of spectral analysis results for two plants with loose thermal shields (reactors A and B) and for a plant of identical design but constructed without a thermal shield (Calvert Cliffs-1). The data were supplied for ex-core neutron detector pairs located 180 deg apart (cross-core detectors) as shown in Fig. 2. Power spectral densities and cross-power spectral density magnitudes of the detector signals were normalized to the mean (dc) signal level squared to produce normalized power spectral densities (NPSD) and normalized cross-power spectral density (NCPSD) magnitudes. These noise descriptors, together with coherences (a measure of signal commonality) and phases between cross-core detectors, were utilized to identify resonant frequencies and mode shapes of reactor internals vibrations.

Reactor A Data Observations

At the beginning of fuel cycle 2 (BOC 2), NPSDs and NCPSDs of cross-core detector signals at reactor A (detectors labeled Safety A and Safety C) exhibit three broad resonances at 3.1, 6.5, and 14.1 Hz as shown in Fig. 5. Coherences were initially high (approximately 0.8) between cross-core detectors over the 3 to 8 Hz region as shown in Fig. 6, and they have a 180 deg phase relationship, which is typical of pendular structural vibrations in the radial plane. The 3.1 Hz resonance is observed in PWRs of similar design and is attributed to fundamental mode fuel assembly vibrations with fixed end conditions (7). Typically, this frequency decreases over a fuel cycle as grid spacer springs relax with radiation damage (8).

With the addition of new fuel assemblies, this resonance usually returns to approximately its beginning-of-cycle frequency. The 6.5 Hz resonance displays these same phase and coherence characteristics but is associated with fuel assembly motion forced by CSB/thermal shield pendular vibrations (9). Typically, this resonance does not shift frequency over the fuel cycle. The 14.1 Hz resonance also exhibits high cross-core detector coherence (0.6 to 0.8) but the phase is approximately 0 deg, which is typical of shell-mode vibrations of the CSB/thermal shield structure (7).

At the BOC 5 in reactor A (the last fuel cycle before thermal shield damage was discovered), the 3.1 and 6.5 Hz resonances had both become sharper and had shifted to 1.5 Hz and 7.5 Hz, respectively, as shown in Fig. 5. Cross-core detector phases remained at 180 deg while coherences were no longer uniformly high over the 3- to 8-Hz range. In this range, isolated resonances became visible in the coherence at 1.5, 4, and 7.6 Hz, as shown in Fig. 6.

The evolution of frequency changes of the 3 Hz resonance is displayed in Fig. 7, versus the fuel cycle for reactor A. Until EOC 3, this resonance behaved similar to that experienced in other PWRs (i.e., decrease in frequency over the fuel cycle due to fuel assembly grid spacer relaxation and increase in frequency at the beginning of the next fuel cycle). After EOC 3, however, this resonance continued to decrease in frequency to 1.5 Hz. This frequency is lower than that normally experienced by other PWRs.

The 6.5 Hz resonance associated with CSB/thermal shield pendular vibrations increased in frequency over the first three fuel cycles of reactor A as shown in Fig. 8. The largest frequency changes (6.5 to 7.7 Hz) occurred over cycles 2 and 3. This increase in frequency is significant since it is in the opposite direction expected for fuel assembly resonant frequency changes. These shifts in frequency are most likely to be the result of changes in the CSB/thermal shield structural dynamics.

The 14.1 Hz resonance associated with CSB/thermal shield shell mode vibrations (Fig. 9) also displayed a decrease in frequency (from 14.1 to 13.3 Hz), occurring primarily during the second and third fuel cycles. Cross-core detector phases were 0 deg at this frequency for all measurements.

Reactor B Data Observations

The ex-core neutron noise from cross-core detector pairs (labeled Safety A and Safety C or Control X and Control Y) at reactor B also displayed high coherence (0.8) over the 3- to 8-Hz region at BOC 1 (Fig. 10). Both pairs of detectors displayed a 180 deg phase relationship. At the BOC 1, resonances were barely visible at 14.1 or 20 Hz in the NPSDs or NCPSDs, and coherences at these frequencies were <0.4.

At the BOC 5 (the last fuel cycle before thermal shield degradation was discovered at reactor B), the coherence in the 14 Hz region had increased to 0.7 and to 0.5 in the 20-Hz region, as shown in Fig. 10. The coherences in the 7 Hz region increased to nearly 1 and a distinct resonance in the coherence could be resolved at 3 Hz. As was observed in reactor A, the 14 Hz resonance decreased to approximately 13 Hz and the 6.3 Hz resonance increased to approximately 7.0 Hz as shown in Figs. 11 and 12 respectively. Phases in the 7.0 Hz region were always 180 deg and 0 deg in the 14 and 20 Hz regions for cross-core detectors.

After fuel cycle 5, damage to the thermal shield supports was discovered at reactor B. During the outage following cycle 5, the thermal shield and its supports were removed. During fuel cycle 6, the reactor operated without a thermal shield. Significant differences were observed between the EOC 5 and EOC 6 cross-core detector coherences, particularly in the 10 to 25 Hz range as shown in Fig. 13. During fuel cycles 5 and 6, signal conditioning and analysis were expanded to include the 25 to 50 Hz frequency range. These results, presented in Fig. 14, show that significant changes in the cross-core detector coherences above 25 Hz occurred when the thermal shield was removed (note that the high coherence appearing at 40 Hz is most likely due to 60 Hz electrical noise aliased by the 100 Hz sampling rate employed in the analysis). This frequency range encompasses higher modes of core internals vibrations.

Comparison of Reactors A and B Data

A comparison between cross-core detector NCPSDs from reactors A and B (Fig. 15) prior to discovery of thermal shield damage indicates that: (1) the resonant frequency associated with pendular CSB motion is higher for reactor A (7.5 Hz) than for reactor B (7 Hz), (2) the resonance associated with shellmode vibrations is lower in frequency for reactor A (13 Hz) and sharper compared to reactor B (14.5 Hz), and (3) a low frequency resonance occurs in the reactor A data at 1.5 Hz which is not visible in the reactor B data. These observations can also be made in the cross-core detector coherences. In addition, coherences of greater than 0.4 occurred in the 12 to 16 and 17 to 21 Hz ranges associated with shell-mode vibrations.

Comparison of Reactor B and Calvert-Cliffs-1 Data

As was previously discussed, the reactor B cross-core detector coherences changed significantly in the 10 to 20 Hz range when the thermal shield was removed. Figure 16 shows a comparison of the cross-core detector coherences between Calvert Cliffs-1 (10) (a CE plant having design similar to reactor B but constructed without a thermal shield) and reactor B without its thermal shield. The coherences are similar below 25 Hz, although the reactor B and Calvert Cliffs data exhibit slight differences in the 12 to 15 Hz range.

INTERPRETATION OF DATA

Based on the previous observations, calculations, and our experience with the behavior of neutron noise in other plants, we made the following interpretations:

- Reactor A and reactor B neutron noise data exhibit frequency shifts in resonances associated with CSB, thermal shield, and fuel assembly structures.

- The changes observed over a fuel cycle in plants with degraded thermal shield supports are abnormal when compared to other plants with or without thermal shields.

- The observed trends in the experimental data (increasing CSB beam mode frequency and decreasing shell mode frequencies) are predicted by finite element model calculations when degraded thermal shield supports are assumed.

- Reactor A data exhibit a low frequency resonance which may be the result of decoupled CSB and thermal shield motions. Since thermal shield vibrations are unlikely to increase neutron noise directly, this resonance may indicate that the thermal shield is impacting the CSB.

- Reactor B data exhibit increases in cross-core detector coherences at two shell-mode frequencies which indicate either increased stimulation of CSB/thermal shield structures or a significant change in their preferential direction (mode shape).

- Reactor A exhibited larger shifts in resonant frequencies than reactor B, indicating a greater change in the structural dynamics prior to discovery of thermal shield damage. This observation was substantiated by the more extensive damage experienced at reactor A compared to reactor B.

- The largest changes in resonant frequencies or cross-core detector coherences occurred during the first or second fuel cycles of both reactors. We hypothesize that this was an indication of thermal shield support degradation early in the life of both plants.

- After the outage for removal of the thermal shield at reactor B, the neutron noise signatures became similar to those of Calvert Cliffs-1, a plant constructed without a thermal shield. This result increases confidence that repair operations were successful and that further damage to the reactor internal structures had not occurred.

RECOMMENDATIONS FOR CORE INTERNALS SURVEILLANCE

As a result of this study, we make the following recommendations for early detection of thermal shield support degradation (including degradation of other internal structures):

- Surveillance of the ex-core neutron noise should, as a minimum, cover the 0- through 50-Hz frequency range.

- Four ex-core detectors, positioned approximately 90 deg apart, should be analyzed to obtain NCPSDs, phases and coherences for all combinations of detector pairs (both cross-core and adjacent).

- Upper and lower sections of ex-core neutron detectors should be analyzed separately, since both experimental and calculated data show an axial dependence of internal vibrations.

- Statistically significant changes or trends in the ex-core neutron noise, particularly changes in the frequency of a resonance, should be considered abnormal until the cause of the change has been identified.

- Ex-core neutron noise should be supplemented with accelerometer measurements since changes in the neutron noise amplitude due to fuel burnup effects (9, 11) may be difficult to interpret. Such measurements would ideally be independent of a LPMS and may require optimal sensor location (i.e., the pressure vessel head flange or surface of the pressure vessel).

- Surveillance of the ex-core neutron noise should be performed periodically: a minimum of once every three months with monthly surveillance being preferred.

- Plants should have a calibrated and operating LPMS. Changes in the neutron noise preceding or existing with impacts detected by the LPMS, indicate the need for immediate diagnostic action. However, a LPMS alone may not be adequate for core internals surveillance because significant structural degradation may have already occurred by the time impacts cause a LPMS alarm.

CONCLUSIONS

Degradation of core internal structures usually involves increases in clearances due to wear or misalignment, or loss of clamping forces. While these changes are inherently small, significant degradation can occur through low amplitude, flow-induced vibrations of large structures. This type of degradation may be difficult to detect visually before the structure's function or integrity are compromised. The failure of the reactor internals in two plants that had undergone 10 year ISI indicates the need for more stringent inspection requirements for reactor internals. In addition, utilities could benefit from standards or guidelines for continuous monitoring of reactor internals similar to the methods outlined in ASME standard OM-5 for loss of CSB axial preload (12).

The results of this study combined with experiences from previous studies, indicate that ex-core neutron noise analysis is a sensitive method for detecting incipient degradation of core internal structures due to flow-induced vibration. Additional applications of this method include verification of structural designs and evaluation of the effectiveness of repairs to reduce flow-induced vibrations. Such techniques could obviously be utilized to monitor the dynamic response of core internal structures with plant life and therefore justify plant life extension.

The effective use of these noise analysis techniques, however, requires that personnel involved in noise data acquisition, analysis, and interpretation have sufficient training and experience to perform their jobs effectively. This experience should be combined with a commitment by the plant or utility to maintain a noise and vibration analysis program over the full life of the plant.

REFERENCES

1. M. P. Paidoussis, "Flow-Induced Vibrations in Nuclear Reactors and Heat Exchangers: Practical Experiences and State of Knowledge," Symposium on Practical Experiences with Flow-Induced Vibrations, Karlsruhe, Federal Republic of Germany, Paper A1, September 3-6 (1979).

2. J. A. Thie, Power Reactor Noise, American Nuclear Society, 1981.

3. D. N. Fry, R. C. Kryter, and J. C. Robinson, "Analysis of Neutron-Density Oscillations Resulting from Core Barrel Motion in a PWR Nuclear Power Plant," Annals of Nuc. Energy 2, 431-351 (1975).

4. C. H. Berlinger and L. E. Phillips, "Loose Parts and Loose Parts Monitoring Systems: The Regulatory Viewpoint," Trans. Amer. Nucl. Soc. 45, 654-655 (1983).

5. W. J. Bryan, "Digital Analysis Techniques Used in Nuclear Fuel Vibration Analysis," ASME Conference on Flow Induced Vibration, San Francisco, p. 91 (June 1979).

6. PAFEC 75 Data Preparation, PAFEC, Ltd., Nottingham, England, (November 1978).

7. D. N. Fry et al., "Neutron Noise in Light-Water Reactors," NUREG/CR-3303, ORNL/TM-8774, Oak Ridge National Laboratory, January 1984.

8. L. A. Walton, F. E. Stokes, and J. N. Black, "Fuel Assembly Dynamic Behavior," Trans. Am. Nucl. Soc. 24, 354 (1976).

9. F. J. Sweeney, J. March-Leuba, and C. M. Smith, "Contribution of Fuel Vibrations to Ex-core Neutron Noise During the First and Second Fuel Cycles of the Sequoyah-1 Pressurized Water Reactor," Prog. in Nucl. Energy 15, 283-290 (1985).

10. J. P. Steelman and B. T. Lubin, "Analysis of Changes with Operating Time in the Calvert Cliffs Unit 1 Noise Signals," Prog. Nucl. Energy 1, 379-391 (1977).

11. F. J. Sweeney and J. P. Renier, "Sensitivity of Detecting In-core Vibrations and Boiling in Pressurized Water Reactors Using Ex-core Neutron Detectors," NUREG/CR-2996, ORNL/TM-8549, Oak Ridge National Laboratory, July 1984.

12. "Inservice Monitoring of Core Support Barrel Axial Preload in Pressurized Water Reactors," ANSI/ASME Standards OM-5-1981.

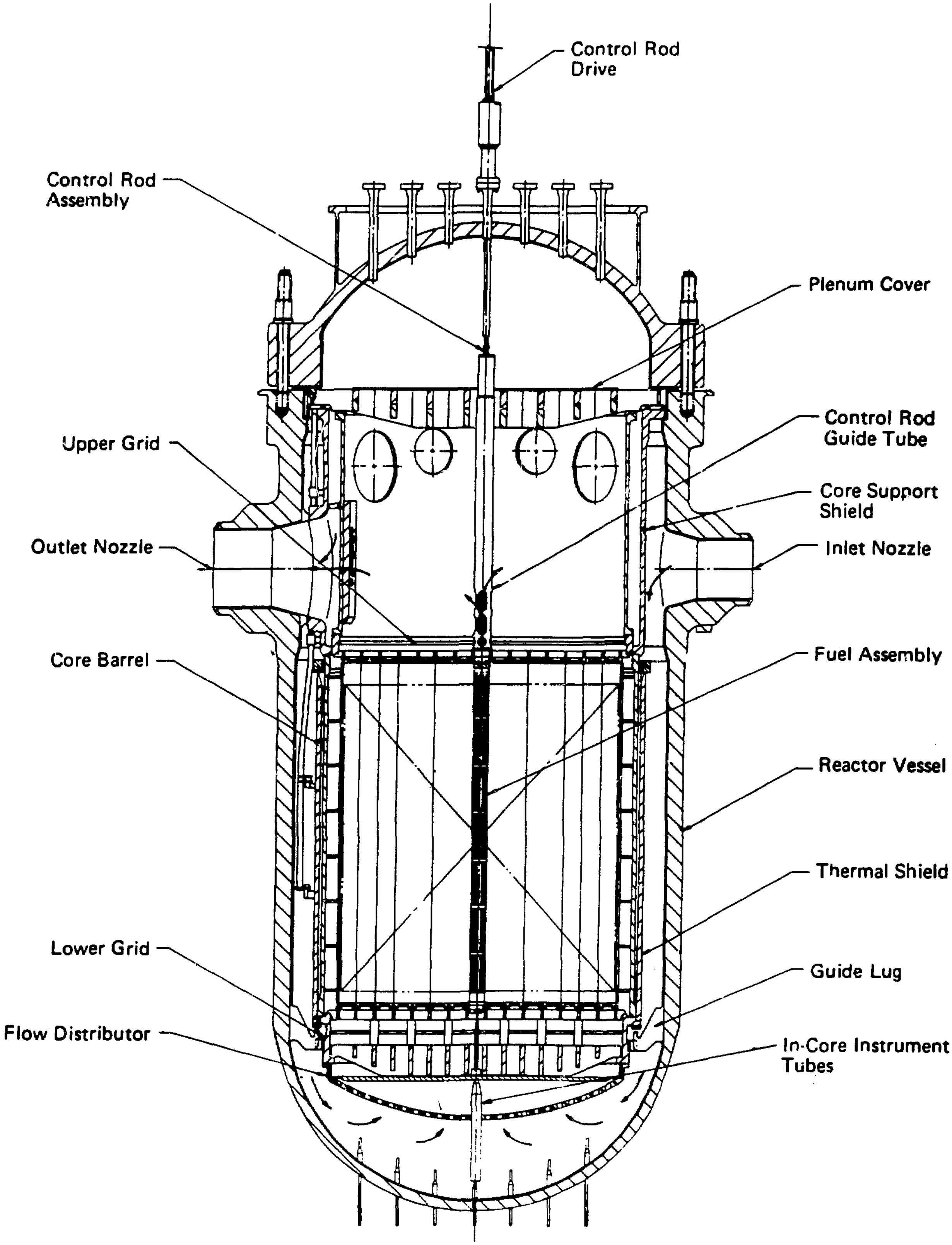

Fig. 1. Cross section of a typical PWR showing internal structures and coolant flow paths.

ORNL-DWG 84-12411

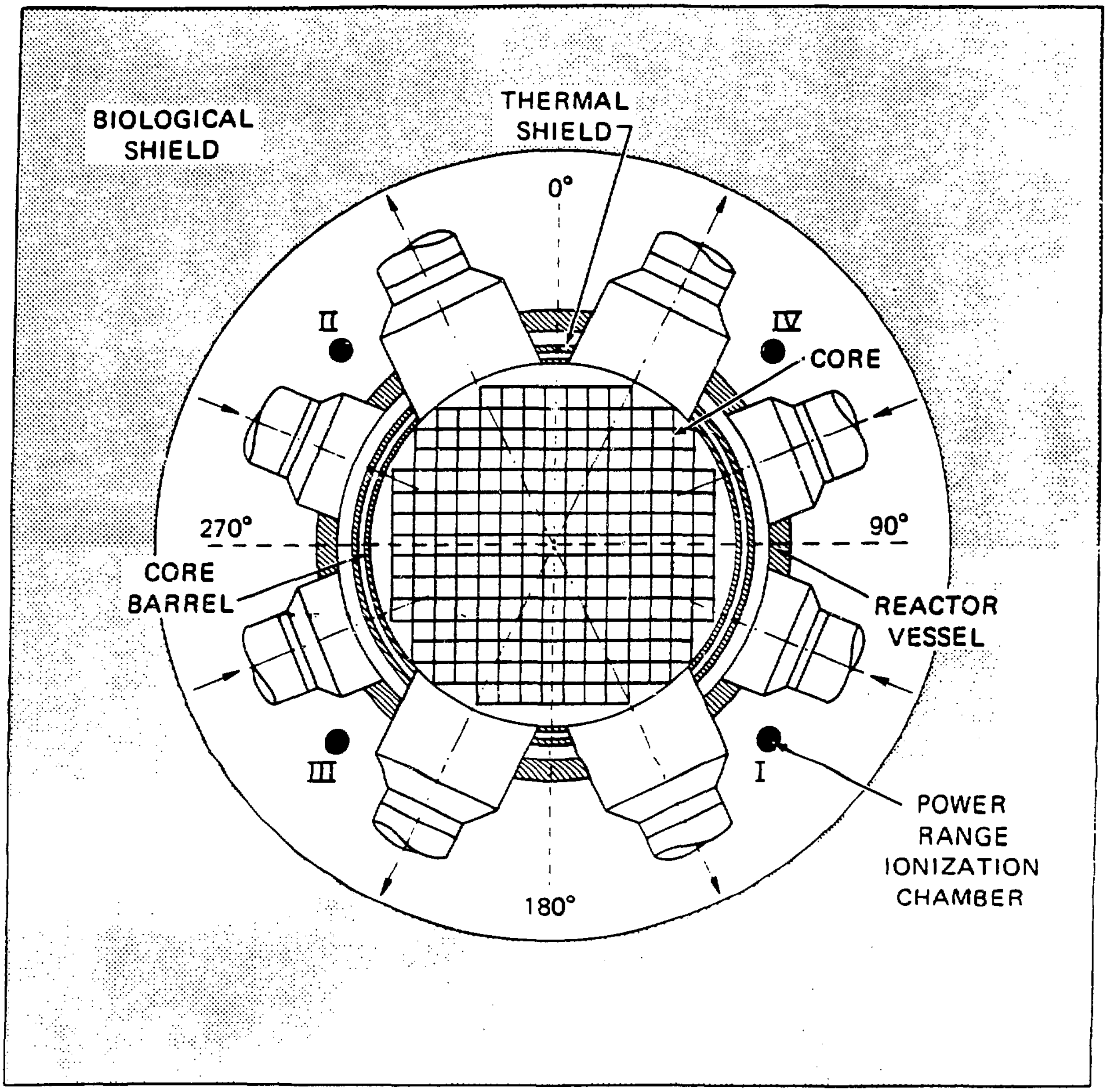

Fig. 2. Cross section of a typical PWR showing location of ex-core detectors relative to core internal structures.

Table 1. Summary of calculated natural frequencies and mode shapes for finite element models of degraded thermal shield supports in a typical PWR

Mode of vibration	Baseline (Hz)	60° Degraded upper attachments (Hz)	No upper attachments (Hz)	No upper attachments, degraded lower attachments (Hz)	No thermal shield (Hz)
Fuel assembly* bending	3.47	3.47	3.47	3.47	3.47
Core barrel and thermal shield beam mode	15.17	15.12	15.03	16.28	16.30
Core barrel and thermal shield shell mode (3 node)	31.2	31.05	36.43	33.54	34.25
Thermal shield shell modes:					
1 node (oval)				3.66	
2 node			22.67	10.88	
3 node			24.00	22.03	

*This frequency was held constant for all cases considered.

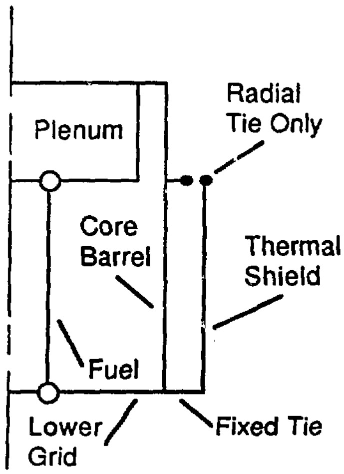

Baseline System

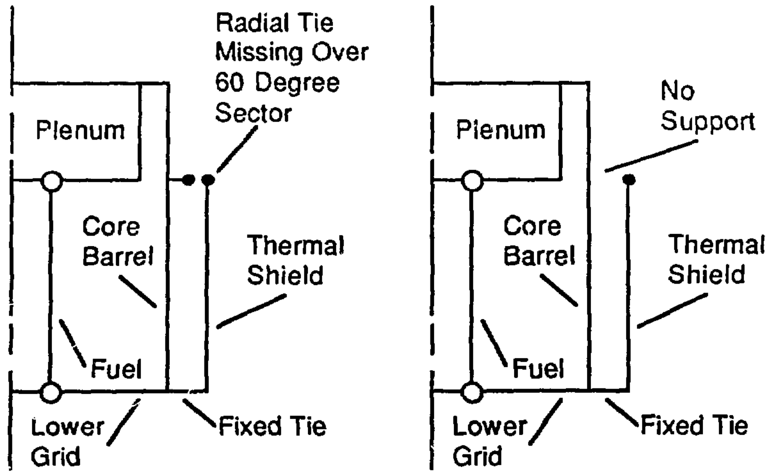

Systems with Degraded Upper Thermal Shield Attachments
(Lower Attachment Fixed)

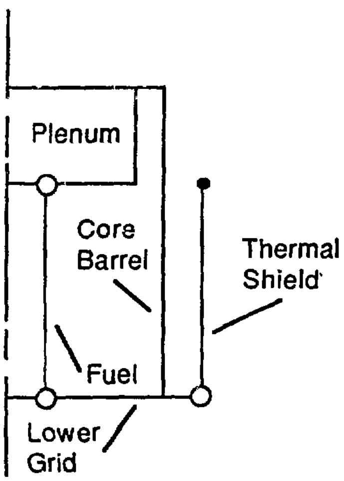

System with Degraded Lower
Thermal Shield Attachment
(No Upper Attachment)

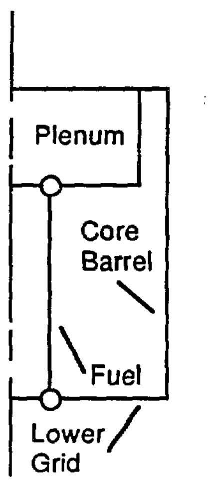

System with No
Thermal Shield

ORNL-DWG 85-14027

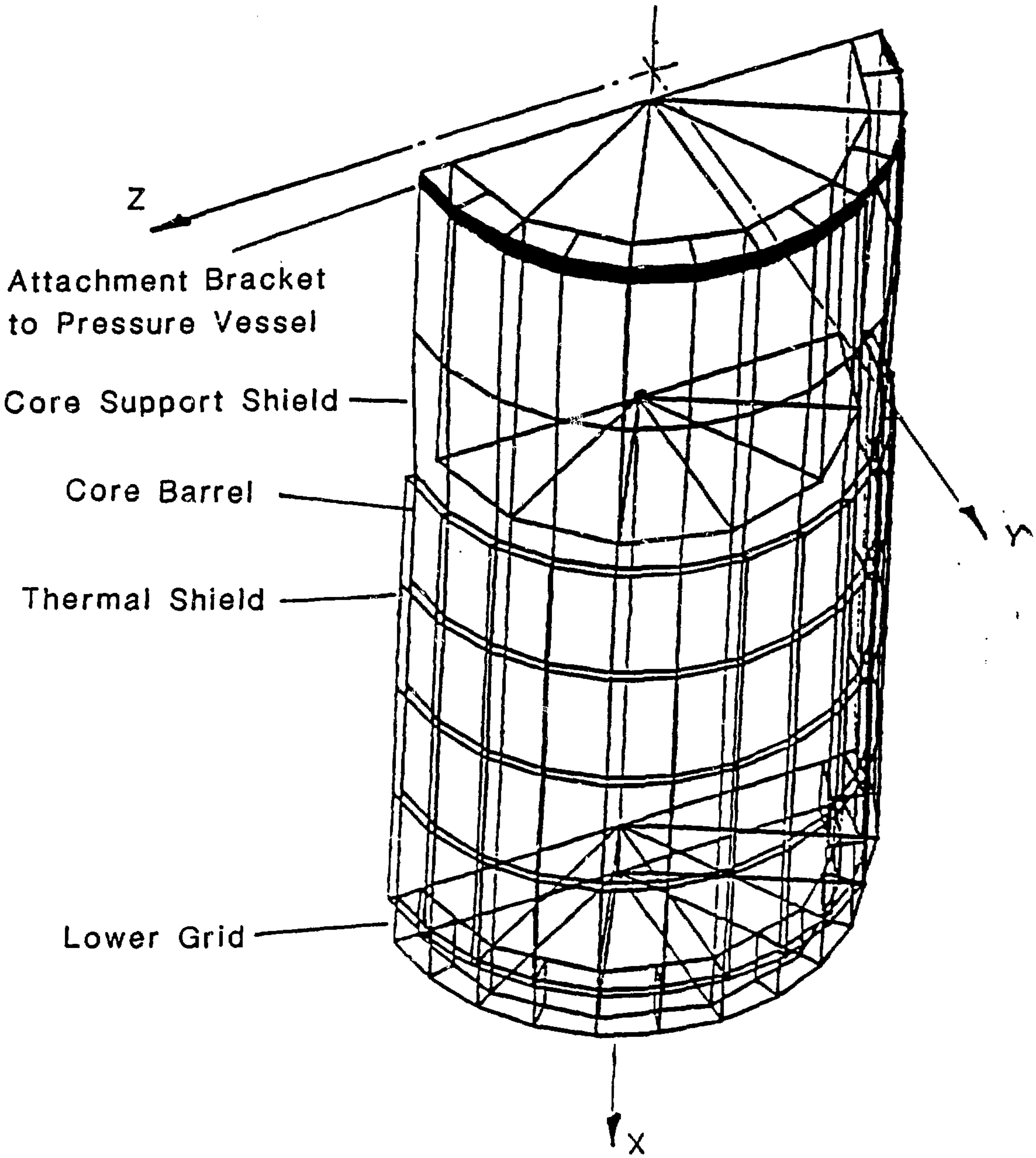

Fig. 3. Finite element model of baseline (undegraded) system with thermal shield.

ORNL-DWG 85-14029

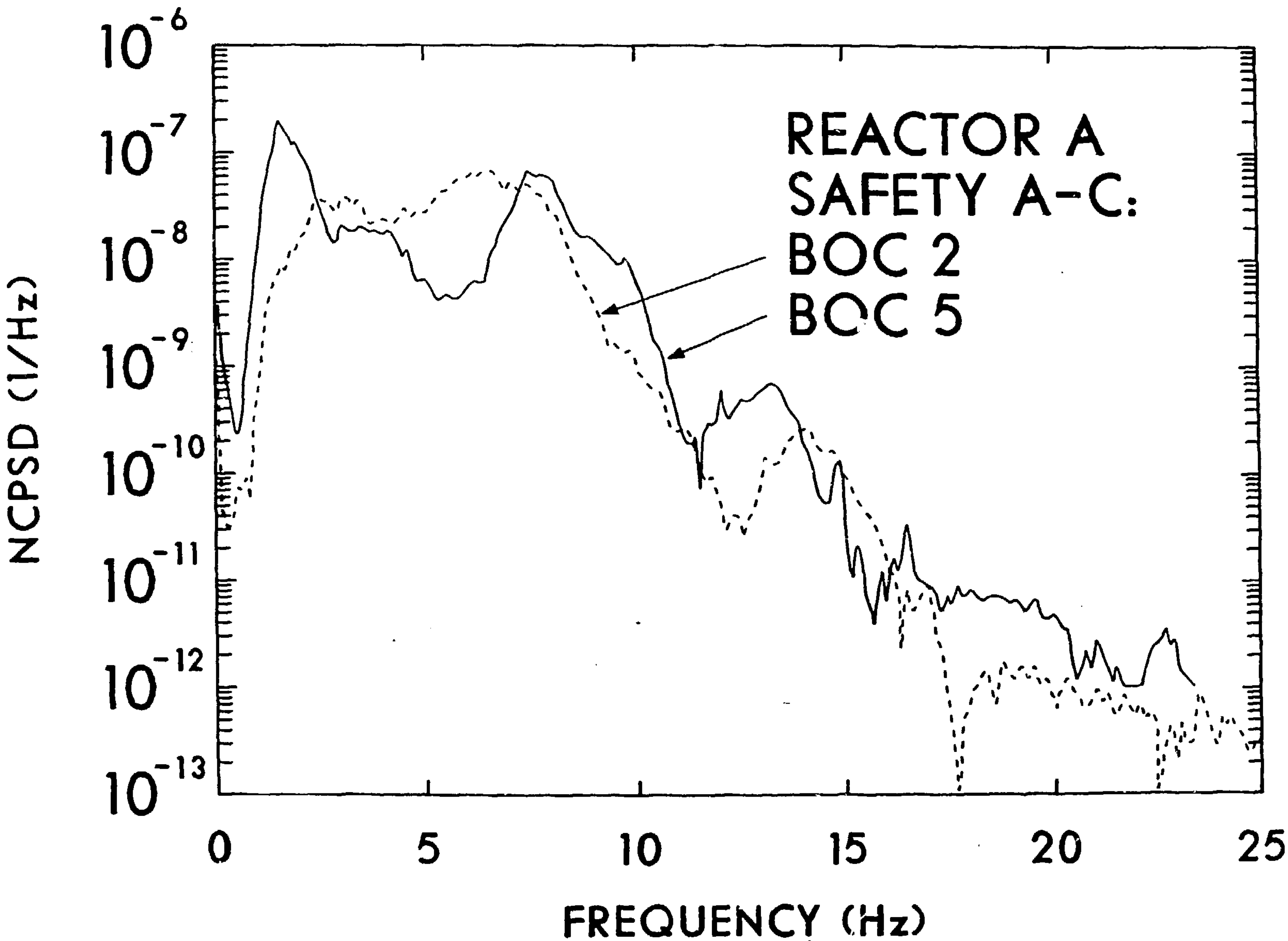

Fig. 5. Normalized cross-power spectral densities (NCPSDs) of cross-core detector pair Safety A and Safety C at Reactor A for beginning of fuel cycles (BOC) 2 and 5 (before thermal sheild removal).

ORNL-DWG 85-14030

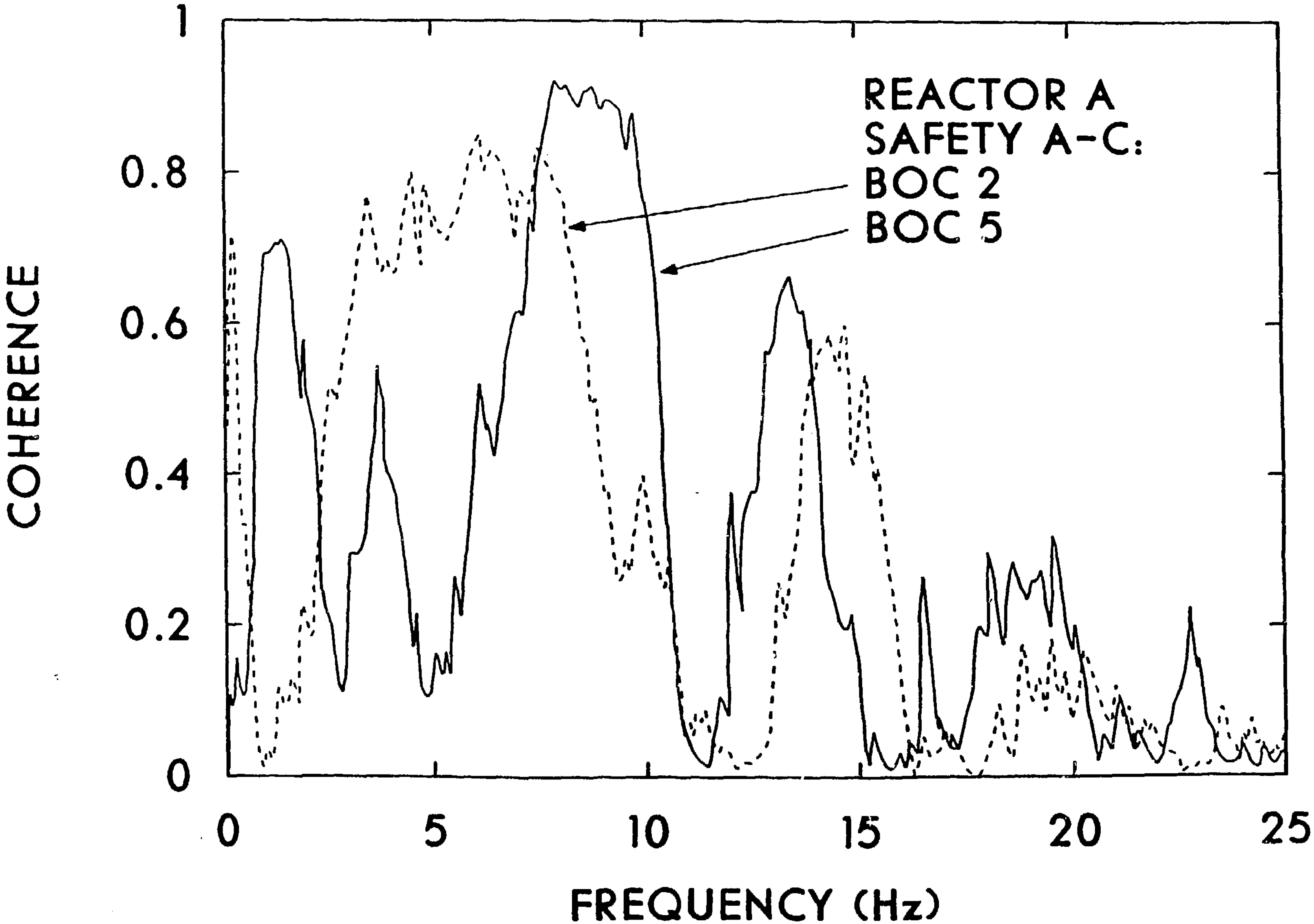

Fig. 6. Coherences for cross-core detector pair Safety A and Safety C at Reactor A for BOC 2 and BOC 5.

ORNL-DWG 85-14031

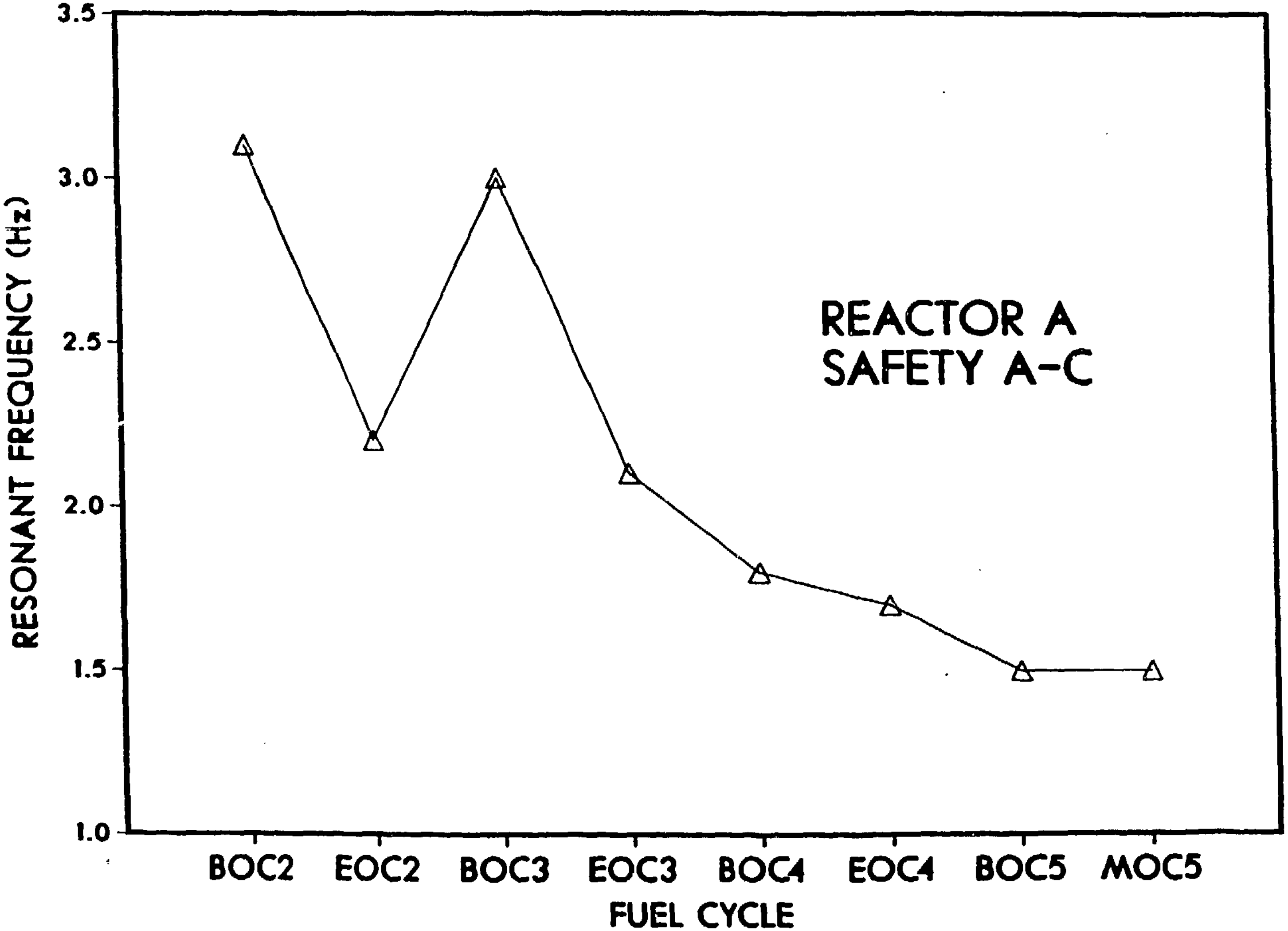

Fig. 7. Frequency evolution of the 3-Hz resonance in the NCPSD of cross-core detector pair Safety A and Safety C at Reactor A.

ORNL-DWG 85-14032

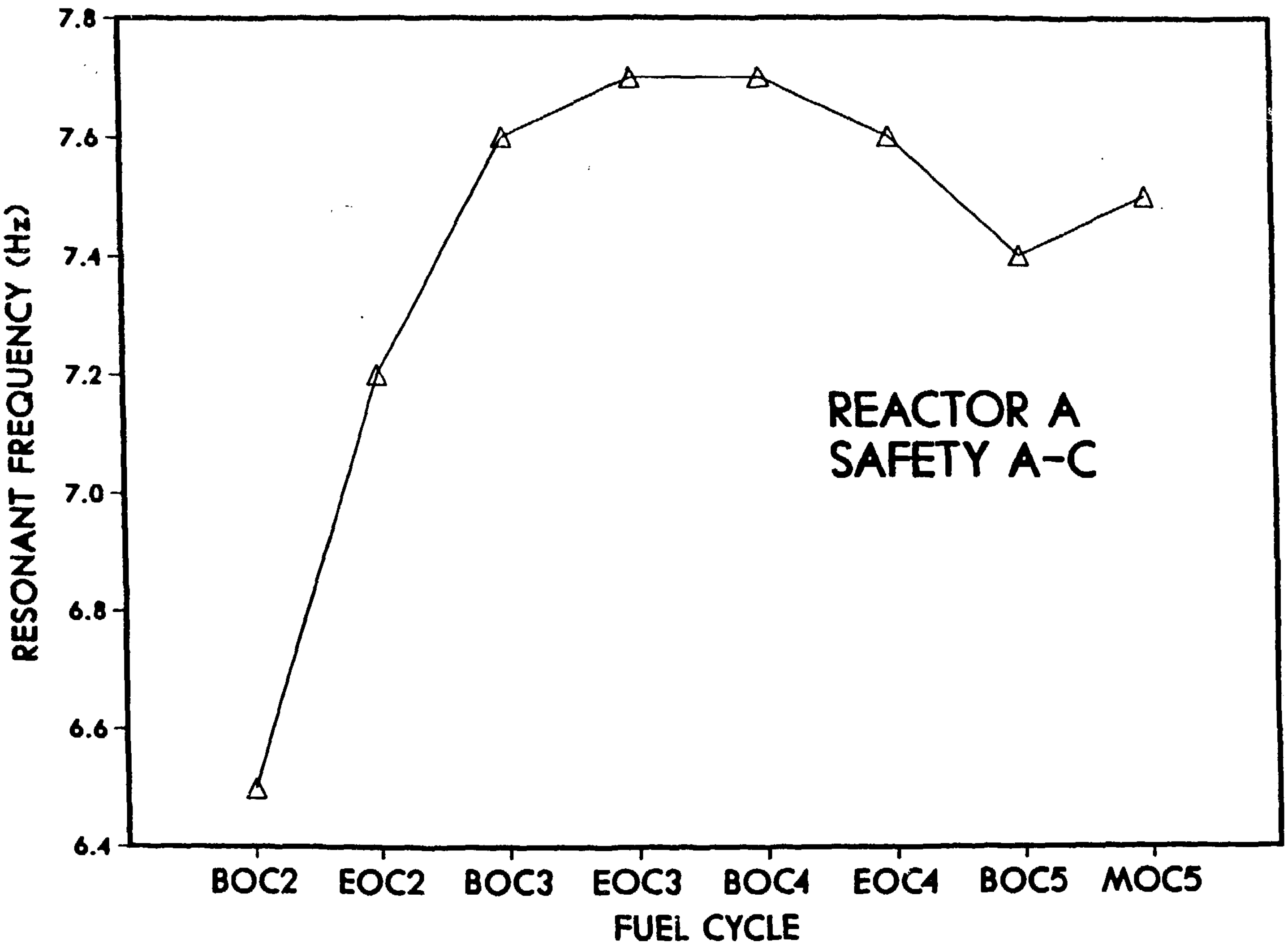

Fig. 8. Frequency evolution of the 6.5-Hz resonance in the NCPSD of cross-core detector pair Safety A and Safety C at Reactor A.

ORNL-DWG 85-14033

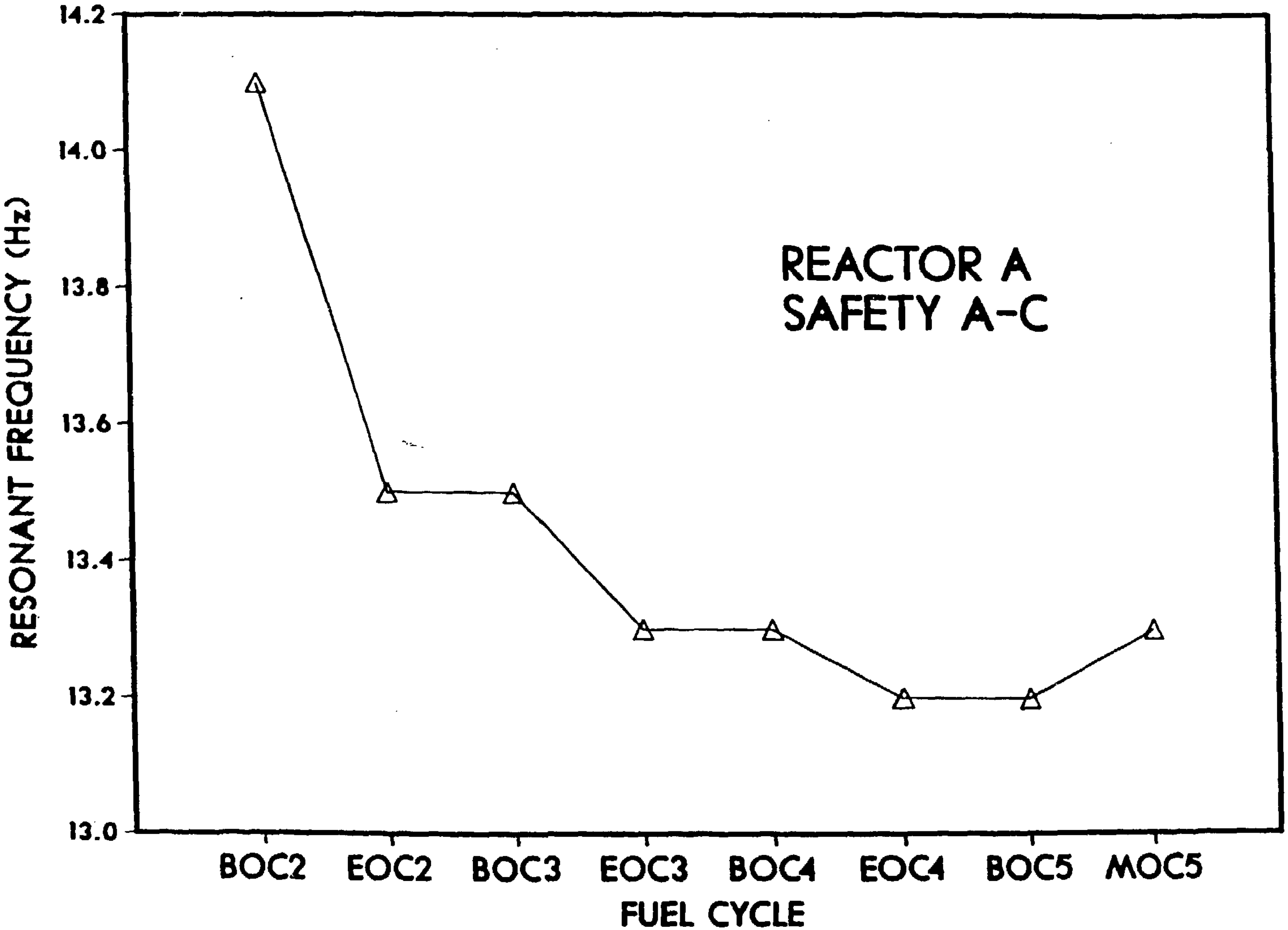

Fig. 9. Frequency evolution of the 14.1-Hz resonance in the NCPSD of cross-core detector pair Safety A and Safety C at Reactor A.

ORNL-DWG 85-14034

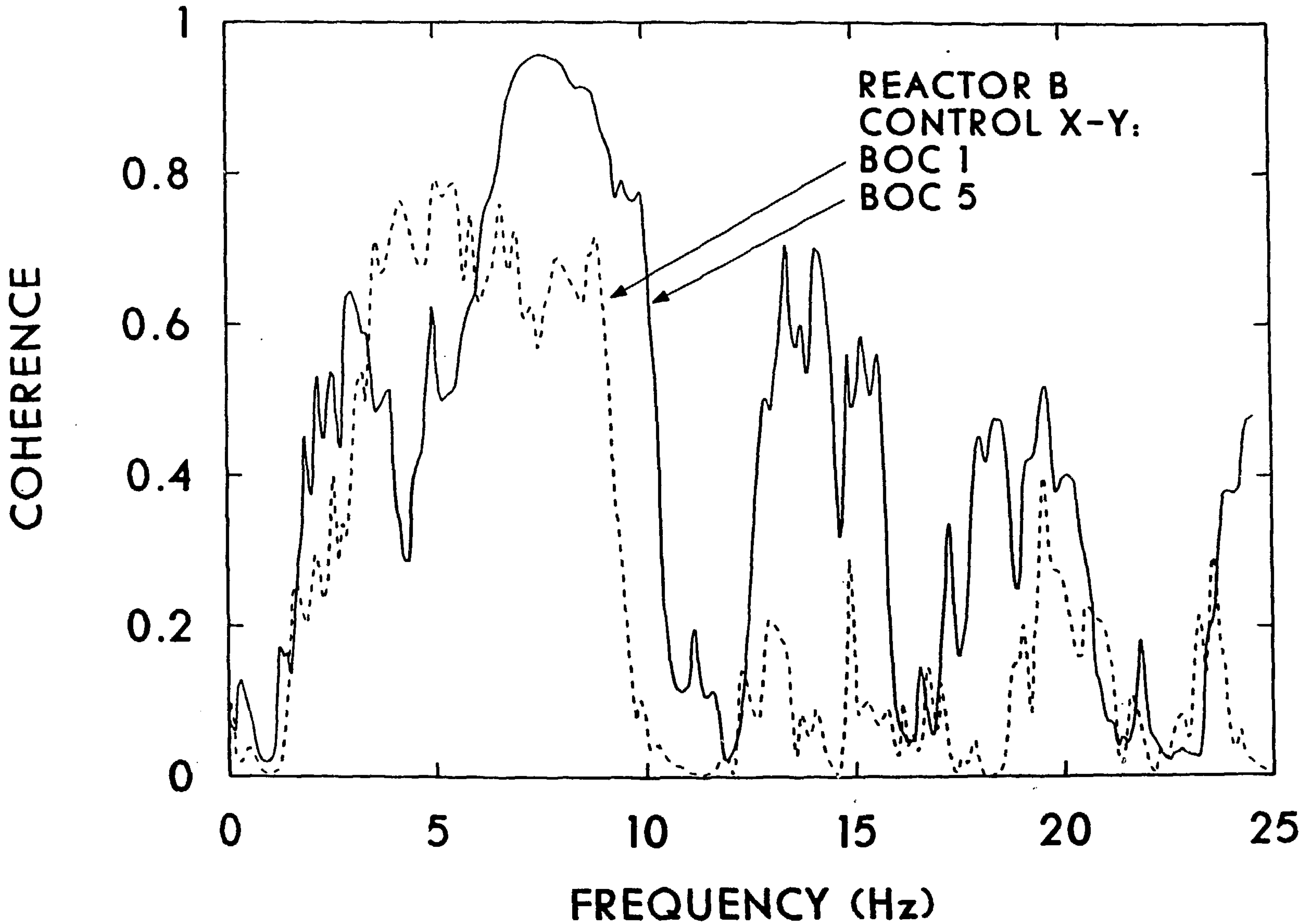

Fig. 10. Coherences between cross-core detector pair Control X and Control Y at Reactor B for BOC 1 and BOC 5.

ORNL-DWG 85-14035

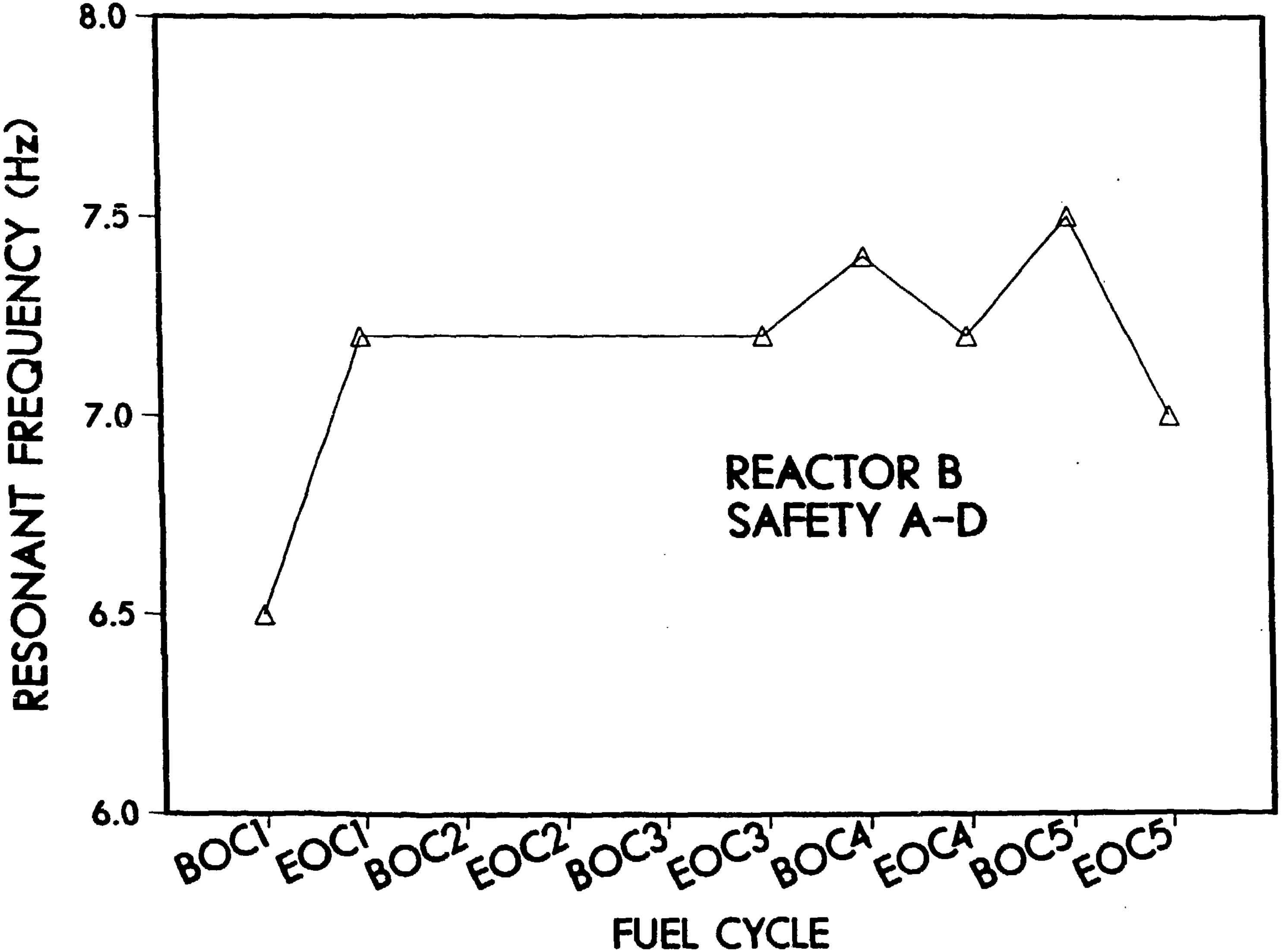

Fig. 11. Frequency evolution of the 6.5-Hz resonance in the NCPSD of cross-core detector pair Safety A and Safety D at Reactor B.

ORNL-DWG 85-14036

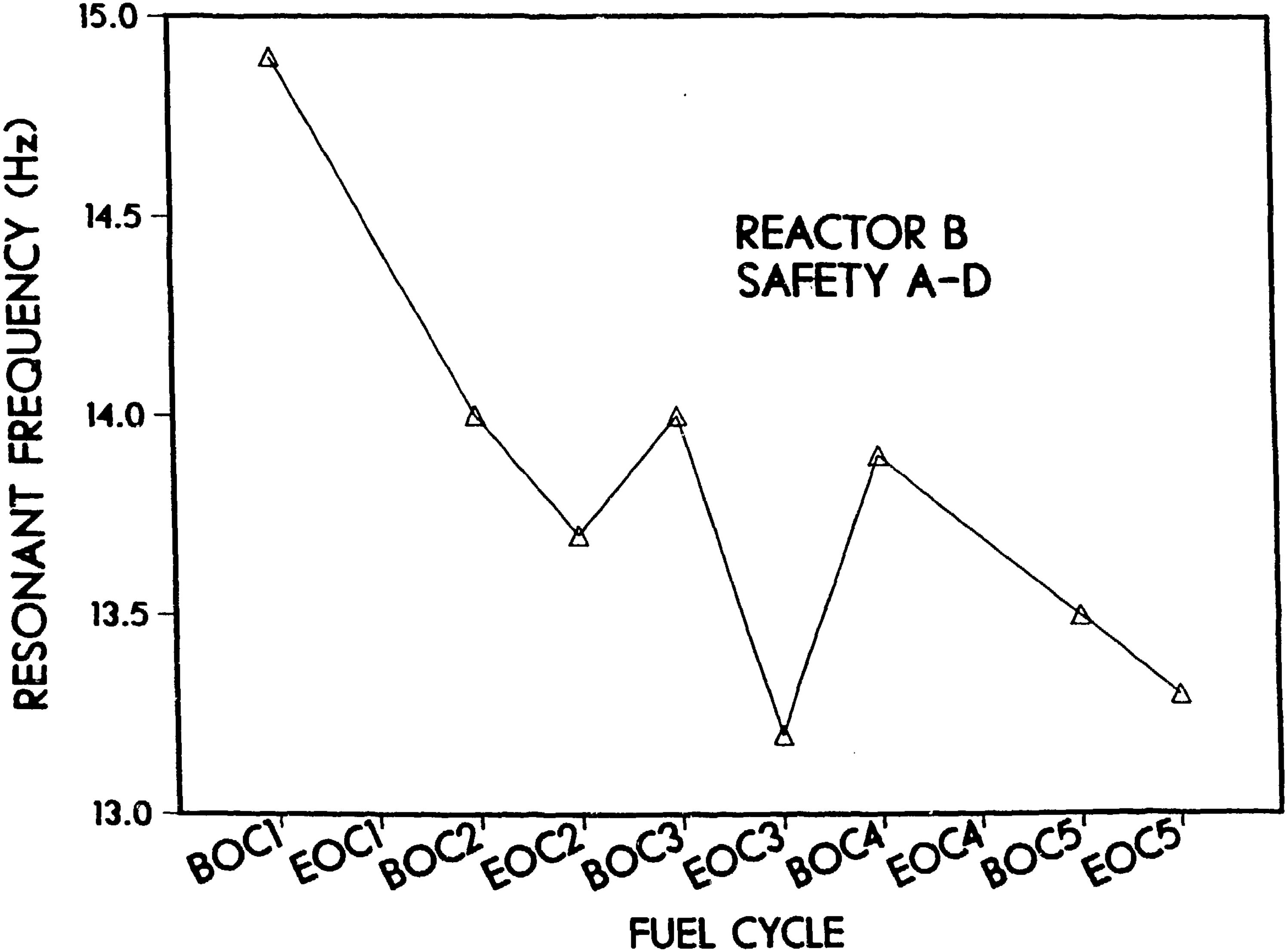

Fig. 12. Frequency evolution of the 14-Hz resonance in the NCPSD of cross-core detector pair Safety A and Safety D at Reactor B.

ORNL-DWG 85-14037

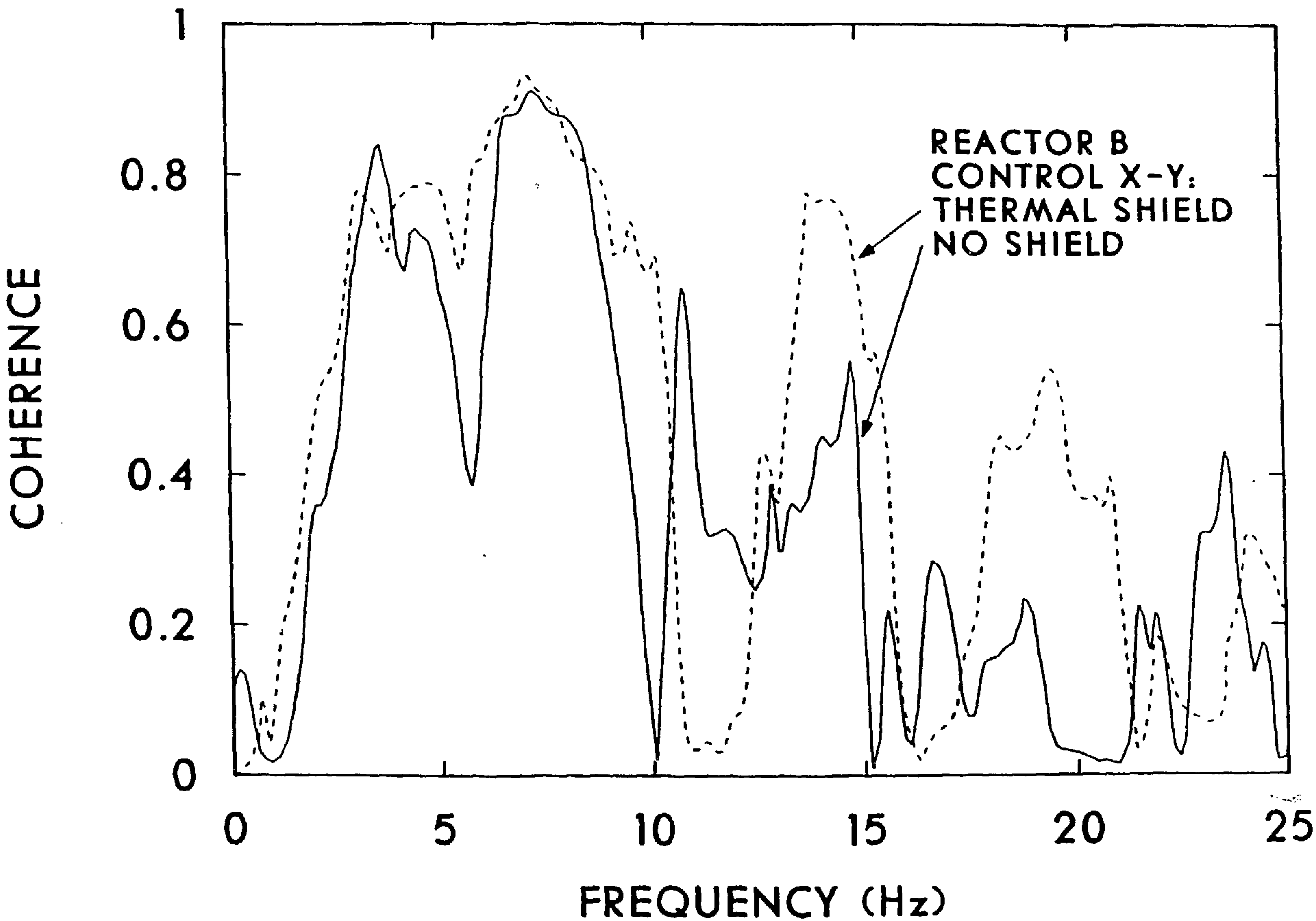

Fig. 13. Coherences between cross-core detector pair Control X and Control Y below 25 Hz at Reactor B for operation with thermal shield (EOC5) and without thermal shield (EOC6).

ORNL-DWG 85-14038

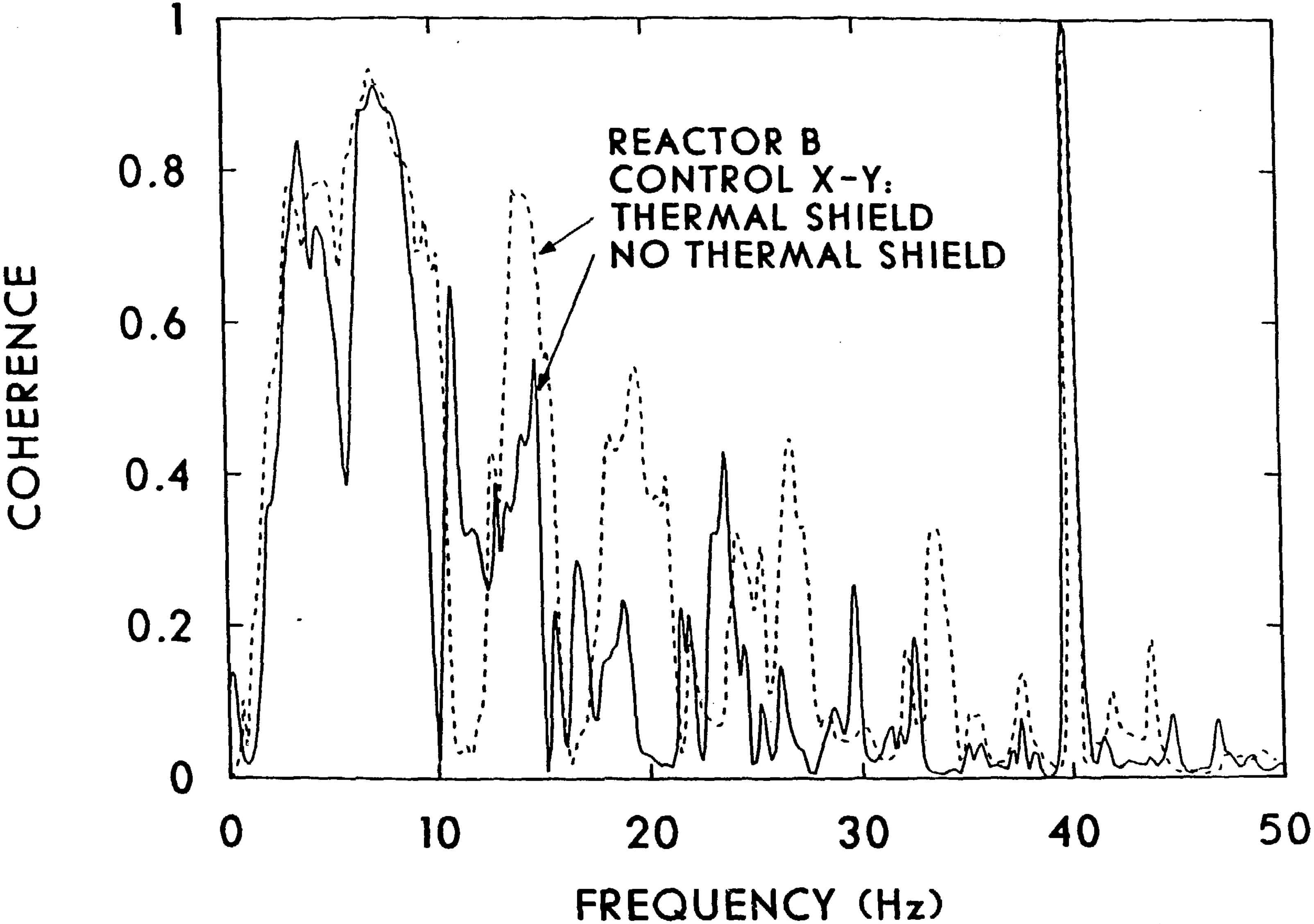

Fig. 14. Coherences between cross-core detector pair Control X and Control Y at Reactor B below 50 Hz for operation with thermal shield (EOC5) and without thermal shield (EOC6).

ORNL-DWG 85-14049

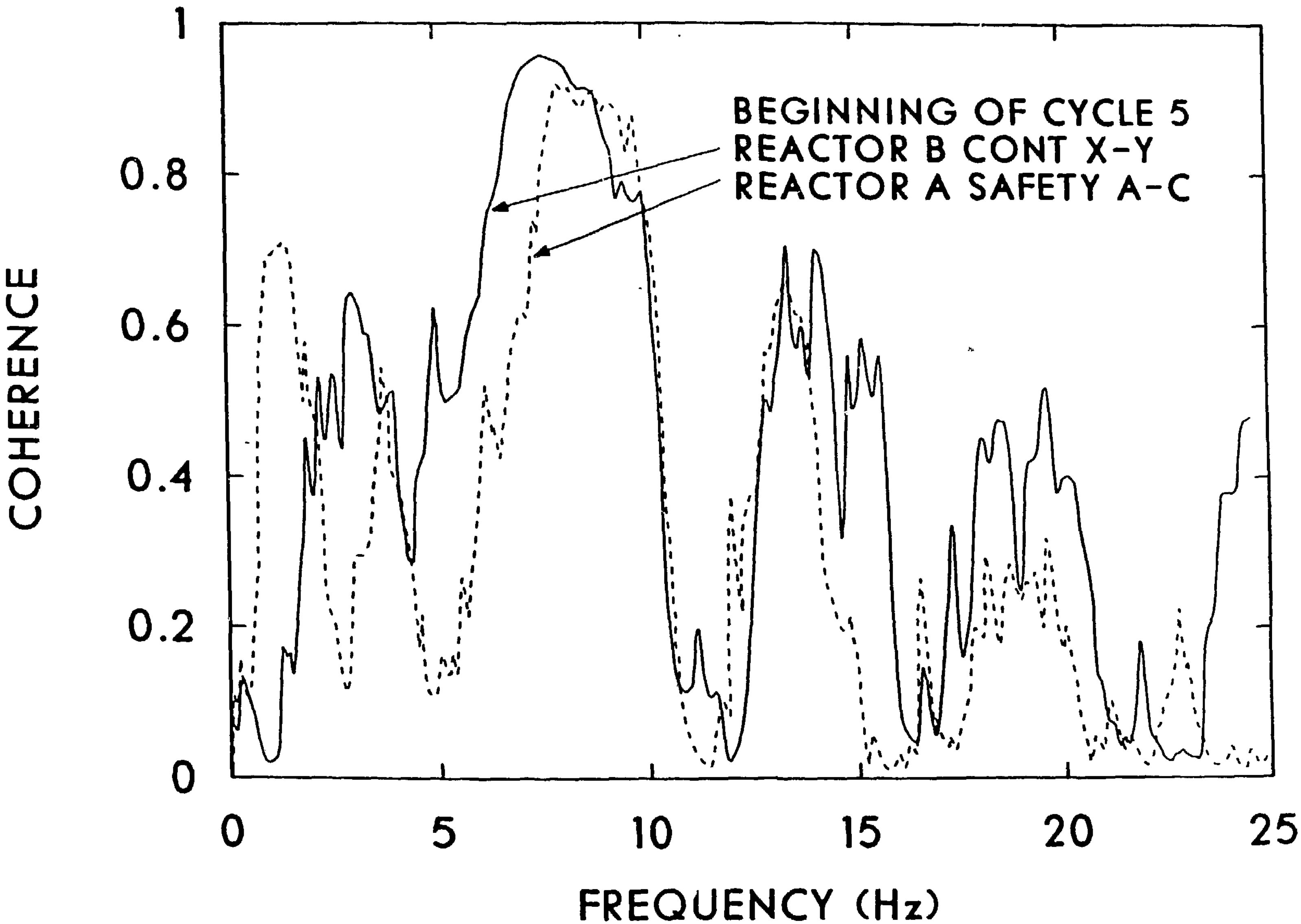

Fig. 15. Comparison of cross-core detector coherence from Reactor A and Reactor B at BOC 5 (prior to the thermal shield removal).

ORNL-DWG 85-14050

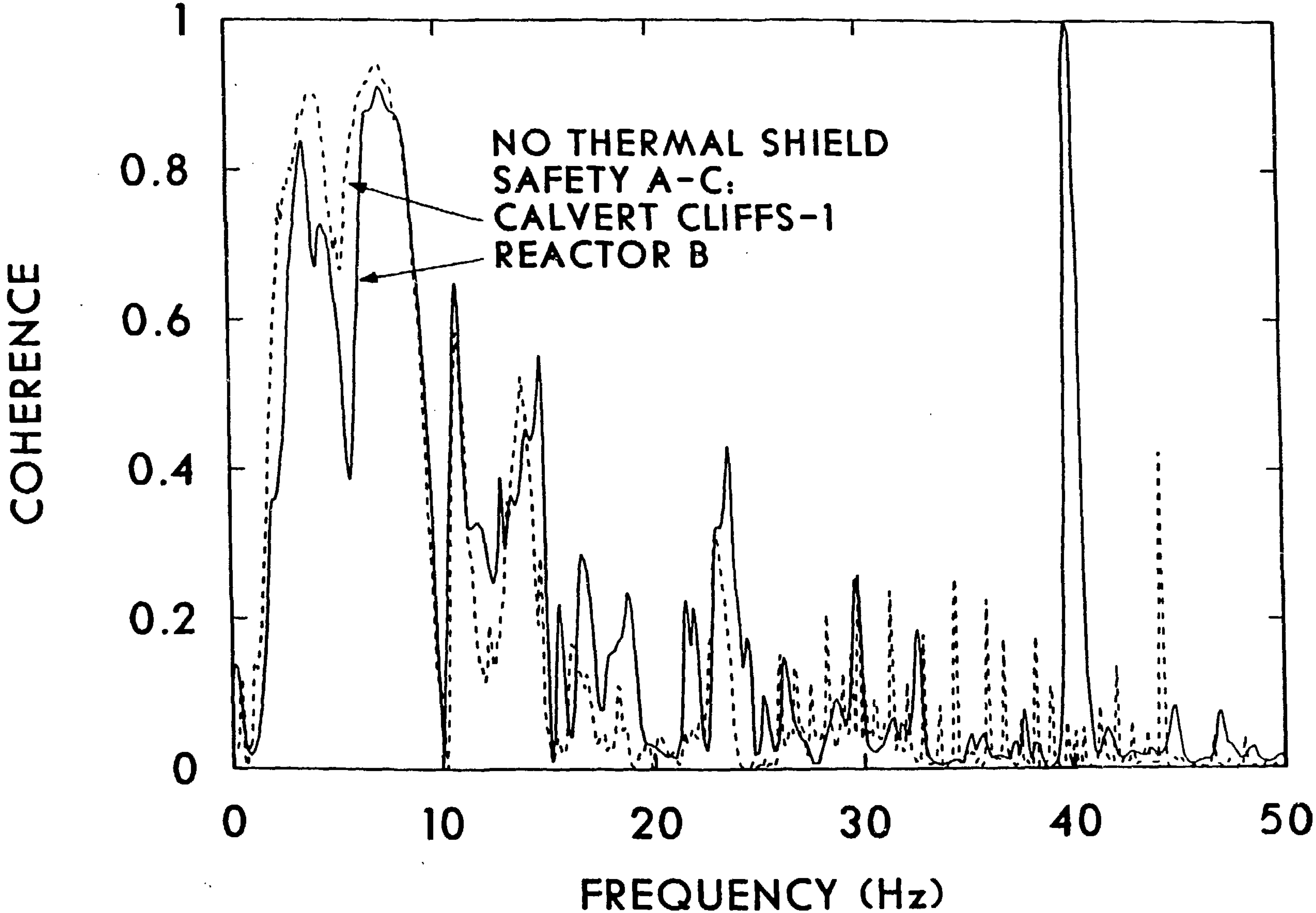

Fig. 16. Comparison of cross-core detector coherences from Reactor B (thermal shield removed) and Calvert Cliffs-1 (constructed without a thermal shield).